Electronic Structure of 3d $[M(H_2O)_6]^{3+}$ Ions from Sc^{III} to Fe^{III}: A Quantum Mechanical Study Based on DFT Computations and Natural Bond Orbital Analyses

Bernd Kallies*,† and Roland Meier*,‡

Institute of Physical and Theoretical Chemistry, University of Potsdam, Karl-Liebknecht-Strasse 24-25, D-14476 Golm, Germany, and Institute of Inorganic Chemistry, University of Leipzig, Talstrasse 35, D-04103 Leipzig, Germany

Received November 14, 2000

The metal−donor atom bonding along the series of 3d $[M(H_2O)_6]^{3+}$ ions from Sc^{3+} to Fe^{3+} has been investigated by density-functional calculations combined with natural localized bond orbital analyses. The $M-OH_2$ bonds were considered as donor−acceptor bonds, and the contributions coming from the metal ion's 3d σ-, 3d π-, and 4s σ-interactions were treated individually. In this way, the total amount of charge transferred from the water oxygen-donor atoms toward the appropriate metal orbitals could be analyzed in a straightforward manner. One result obtained along these lines is that the overall extent of ligand-to-metal charge transfer shows a strong correlation to the hydration enthalpies of the aqua metal ions. If the contributions to the total ligand-to-metal ion charge transfer are divided into σ- and π-contributions, it turns out that Cr^{3+} is the best σ-acceptor, but its π-accepting abilities are the weakest along the series. Fe^{3+} is found to be the best π-acceptor among the 3d hexaaqua ions studied. Its aptitude to accept σ-electron density is the second weakest along the series and only slightly higher than that of Sc^{3+} (the least σ-acceptor of all ions) because of the larger involvement of the Fe^{3+} 4s orbital in σ-bonding. The strengths of the three types of bonding interactions have been correlated with the electron affinities of the different metal orbitals. Deviations from the regular trends of electron affinities along the series were found for those $[M(H_2O)_6]^{3+}$ ions that are subject to Jahn−Teller distortions. In these cases ($d^1 = [Ti(H_2O)_6]^{3+}$, $d^2 = [V(H_2O)_6]^{3+}$, and $d^4 = [Mn(H_2O)_6]^{3+}$), ligand-to-metal charge transfer is prevented to go into those metal orbitals that contain unpaired d electrons. A lowering of the complex symmetry is observed and coupled with the following variations: The $Ti^{3+}-$ and $V^{3+}-$hexaaqua ions switch from T_h to C_i symmetry while the $Mn^{3+}-$hexaaqua ion moves to D_{2h} symmetry. The loss of orbital overlap leading to a diminished ligand-to-metal charge transfer toward the single occupied metal orbitals is compensated by amplified bonding interactions of the ligand orbitals with the unoccupied metal orbitals to some extent.

Introduction

The goal of our present study of the series of 3d $M^{III}-$hexaaqua complexes from $[Sc(H_2O)_6]^{3+}$ to $[Fe(H_2O)_6]^{3+}$ was an improved understanding of the variations in metal-donor atom bonding in relation to the d electron populations of metal ions belonging to this group. The manner in which the bond strength varies among these complexes is related to the concomitant changes of the appropriate hydration enthalpies. Therefore, the relationships between bond strength and hydration enthalpies are studied in detail.

Hexaaqua ions are the archetypes of chelate−metal complexes, and furthermore, in any complex formation reaction in aqueous solution, appropriate $[M(H_2O)_m]^{n+}$ ions are one sort of starting species. Therefore, attainment of a better and more quantitative picture of bonding in the hexaaqua ions can deliver a firm basis for further studies on the interconnectivities between electronic structures of metal complexes and their thermodynamic properties in solution.

It is well-known that the metal−donor atom interactions in that branch of coordination compounds that are commonly regarded as Werner complexes are best described as strongly polar donor−acceptor bonds. The electrostatic character of these bonds has led to the great success of ligand field theory (LFT) to evaluate spectral and magnetic properties.[1−3] The quantity used in the LFT to relate the strength of a ligand field in a transition metal complex to the appropriate complex stability is called ligand field stabilization energy (LFSE). Usually, the LFSE is evaluated from the $10D_q$ parameter that reflects the energy gap between the ground state and first excited state in optical spectra of complexes. In a number of contributions published by Williams[4,5] after the classical paper on the Irving−Williams row of complex stabilities,[6] the author questioned the general validity of the LFSE concept to judge orderings of complex stabilities. He expressed his alerts[5] as follows: "We conclude that the stabilities of complex ions should be referred only to the properties of the ground state and not to $10D_q$." It was also suggested by Williams[4,5] that parameters such as the electron affinities and ionization potentials of the central ions in metal complexes should be the most suitable quantities for the explanation of trends in complex stabilities.

* To whom correspondence should be addressed.
† University of Potsdam.
‡ University of Leipzig.

(1) Schläfer, H. L.; Gliemann, G. *Basic Principles of Ligand Field Theory*; Wiley: New York, 1969.
(2) Ballhausen, C. L. *Introduction to Ligand Field Theory*; McGraw-Hill: New York, 1962.
(3) Jorgensen, C. K. *Modern Aspects of Ligand Field Theory*; Wiley: New York, 1971.
(4) Williams, R. J. P. *J. Chem. Soc.* **1956**, 8.
(5) Williams, R. J. P. *Discuss. Faraday Soc.* **1958**, *26*, 123.
(6) Irving, H.; Williams, R. J. P. *J. Chem. Soc.* **1953**, 3192.

10.1021/ic001258t CCC: $20.00
Published on Web 05/18/2001

In the course of a series of thermodynamic investigations of complex formation reactions of Werner-type complexes in aqueous solution, we had to note that especially the solution thermodynamics of V^{III} complexes shows frequently drastic deviations from the behavior that would be expected from the predictions of the LFSE.[7] Difficulties come into play if the O−M $p_\pi-d_\pi$ donation goes into those metal orbitals where unpaired electrons of the d^2 central ion are accommodated. The queries mentioned above, in connection with the application of the LFSE as a means for assesments of complex stabilities, led us to search for alternative methods for the description of bonding in metal complexes.

During the past decade, ab initio molecular orbital (MO) methods became feasible tools in the analysis of M−L interactions.[8] These techniques are in general less popular than LFT because a lucid interpretation of the primary quantities resulting from computations such as wave functions, electron densities, and canonical molecular orbitals is usually not trivial. One approach by which such results can be transformed into a transparent picture is the natural bond orbital (NBO) formalism, introduced into theoretical chemistry by Weinhold et al.[9] Therefore, the computations using a density-functional theory (DFT) method applied in the present work were followed by a NBO treatment. This approach allows a division of the M−L interactions into electrostatic and charge-transfer contributions. The latter can be further divided into parts belonging to either σ- or π-bonding. On the basis of this technique, a detailed investigation of $M-OH_2$ bonding in hexaaqua complexes of trivalent hexaaqua ions of the 3d series from Sc^{3+} to Fe^{3+} has been carried out.

In the past, various transition metal hexaaqua ions have been investigated by means of quantum mechanical MO methods.[10−16] These calculations have reproduced experimental trends in metal−oxygen distances or hydration energies in a reasonable way. On the basis of Mulliken population analyses and energy partitioning via constrained space orbital variation (CSOV) analyses,[12] it was shown that the M−L interactions in the M^{III}−hexaaqua ions of the 3d series are primarily electrostatic. The dative character of these bonds was estimated to account for less than 10% of the overall interaction energy, but it increases with rising nuclear charge. In this work, we will describe these charge-transfer contributions in more detail. Our analyses benefits from the suitability of the NBO method to partition electron denisties by means of natural localized bond orbitals. Thus, donor−acceptor interactions are identified by deviations of the occupation numbers of localized orbitals that form a particular Lewis structure representation. These deviations can be interpreted as a measure of electron delocalization or resonance. When a purely ionic Lewis structure representation of transition metal complexes is chosen, resonance is similar to the formation of coordinative donor−acceptor bonds.

There are metal ion-dependent differences concerning the extent by which electron densities with σ- or π-character are delocalized along the M−L bonds. The resulting trends will be related to the hydration enthalpies of the naked ions, free solvation enthalpies calculated for the complexes, and electron affinities of metal orbitals. In the first part of our contribution, the structural features of the individual $[M(H_2O)_6]^{3+}$ ions obtained by calculation are compared with experimental geometries. This is followed by a description of the interconnections between the stabilities of these complexes in the gas phase and in water to prove the relationships between the calculated and experimental values for the appropriate hydration enthalpies.

Then, a general description of the nature of the coordinative bonds in the current hexaaqua ions on the basis of the NBO formalism is presented. The extent of transfer of σ- and π-electron density will be related to variations of the complex geometries and thermodynamic data to obtain a consistent and understandable picture of the $[M(H_2O)_6]^{3+}$ complexes. In the last section, we will return to the cases of $[Ti(H_2O)_6]^{3+}$ and $[V(H_2O)_6]^{3+}$, and a detailed analysis of the individual dependencies between charge-transfer and geometric arrangements will be presented.

Computational Details

Density-Functional Calculations. The calculations in the present study have been carried out using the Gaussian 98 program package[17] on an SGI Octane system. The complexes were described in the unrestricted formalism using the Becke3LYP hybrid density functional[18] in combination with a standard 6-31+G* (5d,7f) basis set[17] including all electrons. To avoid SCF convergence problems, a quadratic convergent procedure has been applied. The obtained electron densities were tested to belong to the electronic ground state by swapping occupied and virtual molecular orbitals with d character systematically, followed by reoptimization of the appropriate Kohn−Sham determinant. The state with the lowest energy was used for further calculations.

The Berny algorithm in redundant internal coordinates[19] was applied for geometry optimization of all $[M(H_2O)_6]^{3+}$ model complexes. If possible, the highest molecular symmetry and symmetrical electron densities have been applied during the geometry optimizations. For those ions where Jahn−Teller distortions were expected ($d^1 = [Ti(H_2O)_6]^{3+}$, $d^2 = [V(H_2O)_6]^{3+}$, and $d^4 = [Mn(H_2O)_6]^{3+}$), different molecular symmetries were tested. The stationary points found on the potential energy hypersurfaces as a result of the geometry optimizations for the various molecular symmetries have been tested to represent energy minima rather than saddle points via calculations of analytical force constants based on the harmonic approximation. Unscaled vibrational frequencies were used to obtain the thermal corrections of the total energies via statistical thermodynamics at 298 K and 1 atm.

Electron affinities for the M^{3+} and M^{2+} ions corresponding to the processes expressed in Scheme 1 were estimated with the same DFT

(7) Meier, R.; Boddin, M.; Mitzenheim, S. *Bioinorganic Chemistry: Transition Metals in Biology and their Coordination Chemistry*; Wiley-VCH: Weinheim, 1997; Chapter A-7, p 69.
(8) Frenking, G.; Fröhlich, N. *Chem. Rev.* **2000**, *100*, 717.
(9) Reed, A.; Curtiss, L. A.; Weinhold, F. *Chem. Rev.* **1988**, *88*, 899.
(10) Tachikawa, H.; Ichikawa, T.; Yoshida, H. *J. Am. Chem. Soc.* **1990**, *112*, 982.
(11) Åkesson, R.; Pettersson, L. G. M.; Sandström, M.; Wahlgren, U. *J. Phys. Chem.* **1992**, *96*, 150.
(12) Åkesson, R.; Pettersson, L. G. M.; Sandström, M.; Wahlgren, U. *J. Am. Chem. Soc.* **1994**, *116*, 8691.
(13) Rotzinger, F. P. *J. Am. Chem. Soc.* **1996**, *118*, 6760.
(14) Li, J.; Fisher, C. L.; Chen, J. L.; Bashford, D.; Noodleman, L. *Inorg. Chem.* **1996**, *35*, 4694.
(15) Martin, R. L.; Hay, P. J.; Pratt, L. R. *J. Phys. Chem. A* **1998**, *102*, 3565.
(16) Hartmann, M.; Clark, T.; van Eldik, R. *J. Phys. Chem. A* **1999**, *103*, 9899.
(17) Frisch, M. J.; Trucks, G. W.; Schlegel, H. B.; Scuseria, G. E.; Robb, M. A.; Cheeseman, J. R.; Zakrzewski, V. G.; Montgomery, J. A., Jr.; Stratmann, R. E.; Burant, J. C.; Dapprich, S.; Millam, J. M.; Daniels, A. D.; Kudin, K. N.; Strain, M. C.; Farkas, O.; Tomasi, J.; Barone, V.; Cossi, M.; Cammi, R.; Mennucci, B.; Pomelli, C.; Adamo, C.; Clifford, S.; Ochterski, J.; Petersson, G. A.; Ayala, P. Y.; Cui, Q.; Morokuma, K.; Malick, D. K.; Rabuck, A. D.; Raghavachari, K.; Foresman, J. B.; Cioslowski, J.; Ortiz, J. V.; Stefanov, B. B.; Liu, G.; Liashenko, A.; Piskorz, P.; Komaromi, I.; Gomperts, R.; Martin, R. L.; Fox, D. J.; Keith, T.; Al-Laham, M. A.; Peng, C. Y.; Nanayakkara, A.; Gonzalez, C.; Challacombe, M.; Gill, P. M. W.; Johnson, B. G.; Chen, W.; Wong, M. W.; Andres, J. L.; Head-Gordon, M.; Replogle, E. S.; Pople, J. A. *Gaussian 98*, revision A.7; Gaussian, Inc.: Pittsburgh, PA, 1998.
(18) Becke, A. D. *J. Chem. Phys.* **1993**, *98*, 1372.
(19) Peng, C.; Ayala, P. Y.; Schlegel, H. B.; Frisch, M. J. *J. Comput. Chem.* **1996**, *17*, 49.

Scheme 1. Reactions Defining the Electron Acceptor Potential of Metal 4s (Upper Row) and Metal 3d (Lower Row) Orbitals

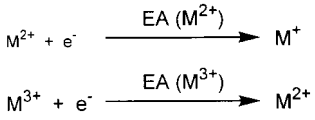

method and basis set as described above by selecting the appropriate electron configurations.

The electronic states of $[Ti(H_2O)_6]^{3+}$ and $[V(H_2O)_6]^{3+}$ have been analyzed in various geometries by state-averaged CASSCF calculations using ROHF/6-31+G* reference functions. The active space included the 3s, 3p, and 3d metal orbitals. The geometries used here were those obtained by partial geometry optimizations with the Becke3LYP/6-31+G* method. The CASSCF calculations were carried out using the MOLPRO 2000 package.[20]

Localization Procedure. The electron densities obtained from DFT computations were transformed into natural localized orbitals with the NBO 4.0 program.[21] A set of bond orbitals (core, lone pairs, two-center σ-orbitals) was selected that corresponds to an ionic resonance structure without covalent metal−ligand bonds. The analyses of the individual electron densities were carried out separately for α (spin-up) and β (spin-down) orientations. The latter reflect the two different opportunities by which a single electron can occupy a metal orbital in terms of the spin direction.

The amount of electron density shifted from the oxygen donor lone pairs (LPs) to the metal ions was judged by means of occupation numbers of the formally unoccupied 3d and 4s orbitals in the NBO basis. A detailed description of how the localization procedure is carried out was given by Weinhold et al.[9] Applications of this method in the analysis of organometallic compounds have been reported recently.[22,23]

Energetic decomposition analyses of the interaction energies into electrostatic, steric, and covalent contributions have not been carried out because the charge-transfer part obtained after deletion of appropriate blocks of elements in the NBO Fock matrices and diagonalization of the new matrices vanished within the error of calculation.

Free Energies of Solvation. The effect of solvation on the $[M(H_2O)_6]^{3+}$ energies by bulk water was estimated by single-point calculations with the polarizable conductor calculation model (PCCM), which is actually an implementation of the COSMO (conductor-like screening model) solvation model[24] in the Gaussian 98 package. This model treats a polar solvent as apparent polarization charges distributed on a molecular cavity like other electrostatic polarizable continuum models, but the boundary condition at the solute/solvent interface is the matching of the solute and solvent electrostatic potentials rather than the electric field.

Radii of interlocking spheres that form the molecular surface were established as follows: Those for oxygen and hydrogen were taken from the united atom topological model (UAHF).[25] The radii of the appropriate M^{3+} ions were extracted from the united force field (UFF).[26] The following individual values have been applied: $r(H_2O) = 1.569$ Å and $r(M^{3+}) = 1.647$ (Sc), 1.587 (Ti), 1.546 (V), 1.511 (Cr), 1.480 (Mn), and 1.456 Å (Fe).

Table 1. Structural Parameters of $[M(H_2O)_6]^{3+}$ Obtained by Calculation and X-ray or Neutron Diffraction

M^{III}	point group calcd	r(M−O), Å		∠(O−M-O′), deg		ϕ, deg	
		exp	calcd[a]	exp[a,b]	calcd[a,b]	exp[a,c]	calcd[a,c]
Sc	T_h	2.070[d]	2.158		90.0		0.0
Ti	C_i	2.025[30]	2.094	90.5	91.5	−20.5	13.6
V	C_i	1.991[34,35]	2.049	91.0	90.6	−20.8	−9.4
Cr	T_h	1.961[36]	2.011	90.8	90.0	−19.0	0.0
Mn	D_2h	1.991[38]	2.038	91.0	90.0	−19.0	0.0
Fe	T_h	1.994[39]	2.050	90.9	90.0	−19.5	0.0

[a] Mean value for complexes without T_h symmetry. [b] Only near rectangular angles reported. [c] Twist angle defining the orientation of the water planes relative to the MO_6 core, see text for definition. [d] Taken from ref 12 without proof.

These values were scaled by 1.2 to allow for the variation of the dielectric from its bulk value to the solute/solvent boundary. The CPCM implementation in Gaussian 98 also includes nonelectrostatic contributions to the free energy of solvation. The dependence of the cavitation energy on the surface area of the solute was calculated according to the method developed by Pierotti.[27] Short-range solute/solvent dispersion and repulsion terms were considered as suggested by Tomasi and Floris.[28]

Results and Discussion

Basic Features of the $[M(H_2O)_6]^{3+}$ Arrangements. The solid-state structures of 3d $[M(H_2O)_6]^{3+}$ ions have been studied by X-ray and neutron diffraction measurements in various environments.[29] Individual structural studies of hexaaqua ions that are the subject of the present paper have been communicated for M = Ti,[30−32] V,[33−35] Cr,[36,37] Mn,[38] and Fe.[39] Among the extensively studied alum structures of the type $M'[M^{III}(H_2O)_6]\cdot 6H_2O\cdot 2SO_4$, those with Cs^+ as a counterion are most relevant to our results. Thus, the calculated geometric features of the hexaaqua ions (minimum energy structures at the Becke3LYP/6-31+G* level at 0 K in the gas phase) are compared in Table 1 with the corresponding data from neutron diffractional investigations of $Cs[M^{III}(H_2O)_6]\cdot 6H_2O\cdot 2SO_4$ structures.

Quantum mechanical calculations on these systems with a variety of methods (UHF, DFT, CASSCF, or CI with effective core potentials or all-electron split valence basis sets including polarization and diffuse functions) have been reported for M = Sc to Fe,[12] M = Ti,[10,13,16] M = Cr or Mn,[11] M = Mn or Fe,[14] and M = Fe.[15]

At the beginning of the discussion of our results, we will present a brief review of the geometric arrangements that can

(20) MOLPRO is a package of ab initio programs written by H.-J. Werner and P. J. Knowles, with contributions from R. D. Amos, A. Berhardsson, A. Berning, P. Celani, D. L. Cooper, M. J. O. Deegan, A. J. Dobbyn, F. Eckert, C. Hampel, G. Hetzer, T. Korona, R. Lindh, A. W. Lloyd, S. J. McNicholas, F. R. Manby, W. Meyer, M. E. Mura, A. Nicklass, P. Palmieri, R. Pitzer, G. Rauhut, M. Schütz, H. Stoll, A. J. Stone, R. Tarroni, and T. Thorsteinsson.
(21) Glendening, E. D.; Badenhoop, J. K.; Reed, A. E.; Carpenter, J. E.; Weinhold, F. *NBO 4.0*; Theoretical Chemistry Institute, University of Wisconsin: Madison, 1996.
(22) Landis, C. R.; Firman, T. K.; Root, D. M.; Cleveland, T. *J. Am. Chem. Soc.* **1998**, *120*, 1842.
(23) Kaupp, M. *Chem. Eur. J.* **1999**, *5*, 3631.
(24) Barone, V.; Cossi, M. *J. Phys. Chem. A* **1998**, *102*, 1995.
(25) Barone, V.; Cossi, M. *J. Chem. Phys.* **1997**, *107*, 3210.
(26) Rappé, A. K.; Casewit, C. J.; Colwell, K. S.; Goddard, W. A., III; Skiff, W. M. *J. Am. Chem. Soc.* **1992**, *114*, 10024.
(27) Cossi, M.; Barone, V.; Cammi, R.; Tomasi, J. *Chem. Phys. Lett.* **1996**, *255*, 327.
(28) Cossi, M.; Mennucci, B.; Cammi, R. *J. Comput. Chem.* **1996**, *17*, 57.
(29) Beattie, J. K.; Best, S. P. *Coord. Chem. Rev.* **1997**, *166*, 391.
(30) Tregenna-Piggott, P. L. W.; Best, S. P.; O'Brien, M. C. M.; Knight, K. S.; Forsyth, J. B.; Pilbrow, J. R. *J. Am. Chem. Soc.* **1997**, *119*, 3324.
(31) Aquino, M. A. S.; Clegg, W.; Liu, Q. T.; Sykes, A. *Acta Crystallogr.* **1995**, *C51*, 560.
(32) Sygusch, J. *Acta Crystallogr.* **1982**, *B24*, 1968.
(33) Cotton, F. A.; Fair, C. K.; Lewis, G. F.; Mott, G. N.; Ross, F. K.; Schultz, A. J.; Williams, J. M. *J. Am. Chem. Soc.* **1984**, *106*, 5319.
(34) Beattie, J. K.; Best, S. P.; Del Favero, P.; Skelton, B. W.; Sobolev, A. N.; White, A. H. *J. Chem. Soc., Dalton Trans.* **1996**, 1481.
(35) Tregenna-Piggott, P. L. W.; Best, S. P.; Güdel, H. U.; Weihe, H.; Wilson, C. C. *J. Solid State Chem.* **1999**, *145*, 460.
(36) Best, S. P.; Forsyth, J. B. *J. Chem. Soc., Dalton Trans.* **1991**, 1721.
(37) (a) Schein, J. B.; Lingafelter, E. C.; Stewart, J. M. *J. Chem. Phys.* **1967**, *47*, 5183. (b) Spichiger, D.; Carver, G.; Dobe, C.; Bendix, J.; Tregenna-Piggott, P. L. W.; Meier, R.; Zahn, G. *Chem. Phys. Lett.*, **2001**, *337*, 391.
(38) Beattie, J. K.; Best, S. P.; Skelton, B. W.; White, A. H. *J. Chem. Soc., Dalton Trans.* **1981**, 2105.
(39) Best, S. P.; Forsyth, J. B. *J. Chem. Soc., Dalton Trans.* **1990**, 3507.

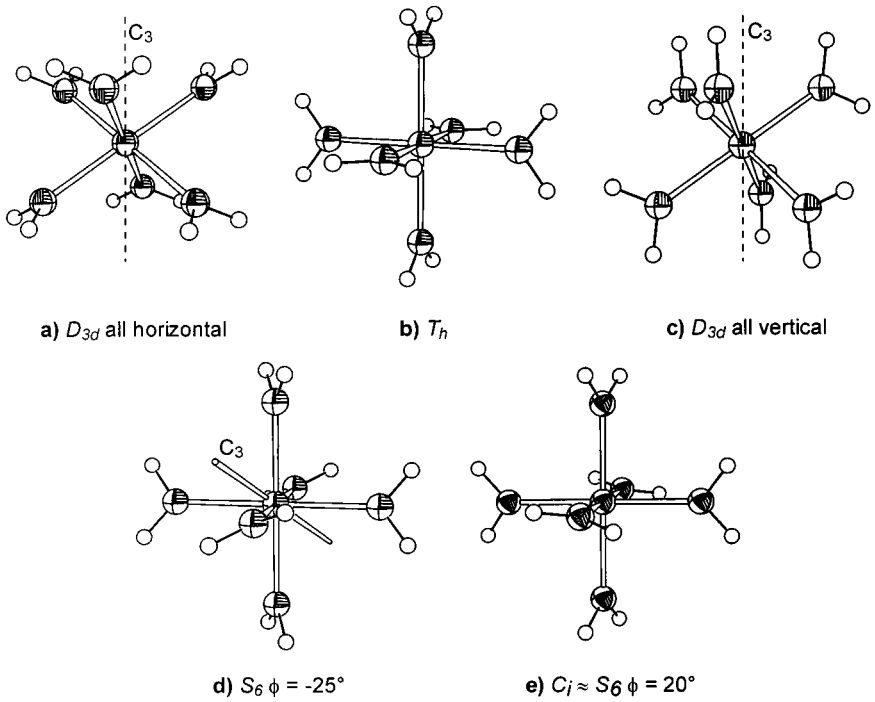

Figure 1. Studied conformations of $[Ti(H_2O)_6]^{3+}$ and $[V(H_2O)_6]^{3+}$ with planarly ligating water molecules.

be adopted by hexaaqua ions where the coordinated water molecules are planarly arranged. According to crystal field theory (optimal electrostatic interactions and minimal steric strain resulting from ligand−ligand interactions in a hexaaqua ion), the symmetry adopted by a 3d M^{III} hexaaqua ion should be T_h (cf. Figure 1b). This arrangement is characterized by O_h symmetry of the MO_6 core.

Generally, a ligand field with T_h symmetry induces a splitting of five degenerated d orbitals into three t_g and two e_g orbitals. This leads to degenerated ground states for d^1, d^2, and d^4 (high-spin) systems. Therefore, T_h symmetry should only be favored in those $[M(H_2O)_3]^{6+}$ ions with a d^0 (Sc^{III}), d^3 (Cr^{III}), and d^5 high-spin (Fe^{III}) d electron configuration. For hexaaqua ions with uneven occupation of the t_g or e_g subshells (Ti^{III}, V^{III}, Mn^{III}), the Jahn−Teller theorem predicts a lowering of the complex symmetry.

As discussed in detail by Cotton et al.,[33] during the neutron diffraction structural study of $[V(H_2O)_6][H_5O_2](CF_3SO_3)_4$, electronic influences could modify the arrangements of ligands in hexaaqua ions with d^1 and d^2 electron configurations as shown with structures in Figure 1, panel a (D_{3d}, all horizontal) and c (D_{3d}, all vertical). The transformation from T_h symmetry (Figure 1b) into the arrangements shown in Figure 1a,c is induced by rotations of the H−O−H planes about the M−O axes. The extent of deviation from T_h symmetry is measured with the twist angle ϕ that is defined as the dihedral angle between the plane of a water molecule and the closer MO_4 plane that includes its oxygen atom. The sign of ϕ is referred to the C_3 axis of the MO_6 octahedron that corresponds to the symmetry axis of the D_{3d} structures. The angle ϕ takes the values:[29] T_h, $\phi = 0°$; D_{3d}, all horizontal, $\phi = -45°$; and D_{3d}, all vertical, $\phi = 45°$. Along the pathways from T_h into both the limiting D_{3d} arrangements, various structures with S_6 symmetry are traversed (Figure 1e). The O_h symmetry of the MO_6 core is retained along these paths. The D_{3d} arrangements are not confined to O_h symmetry of MO_6. They are allowed to become compressed or elongated along the C_3 axis. In addition, the water dipoles do not have to point directly toward the central ion. Additional geometrical variables are required to describe these structures in detail. A symmetry lowering of the intermediate S_6 arrangements can also be induced by angular distortion of the MO_6 octahedron, reaching the C_i point group (Figure 1d) eventually.

A different kind of symmetry lowering from T_h is expected for the d^4 ion $[Mn(H_2O)_6]^{3+}$ because of the ^5E_g (T_h) gound state of the naked central ion. Either axial compression or elongation should take place leading to a D_{2h} symmetric structure (with or without D_{4h} symmetry of the MO_6 core).

It becomes visible from data in Table 1 that our geometry optimizations lead to the expected minima with T_h symmetry anticipated for the hexaaqua ions with d^0, d^3, and d^5 configurations. Deviations from T_h were encountered with the d^1, d^2, and d^4 ions as well.

As expected, two D_{2h} structures are found for $[Mn(H_2O)_6]^{3+}$ by using restricted basis sets and the UHF method, showing an energy difference of about 1 kcal/mol at the UHF/6-31+G* level, with a preference for the axially elongated structure. Similar findings were already reported by Åkesson et al.[11] Within the method used for final results, only the tetragonally elongated structure exists as a stationary point. In the case of Ti^{III} and V^{III}, T_h and the D_{3d} symmetrical arrangements represent transition states of higher order. The imaginary frequencies describe coupled rotations of the water planes about the M−O bonds. As a result of a continuous lowering of the symmetry, we find C_i structures representing potential energy minima for the d^1 and d^2 aqua ions in the gas phase at 0 K (see Table 2). These findings differ from the predictions by Cotton et al.,[33] who suggested the preference of the d^1 and d^2 ions for D_{3d} all-vertical and D_{3d} all-horizontal arrangements, respectively. The basis of these suggestions was the shape of the V^{III} hexaaqua unit in $[V(H_2O)_6][H_5O_2](CF_3SO_3)_4$, which is nearly D_{3d} all horizontal. In this way, optimal V−O π-bonding can be realized with concomitant adhering to the Jahn−Teller requirements. The latter statement was supported by Fenske−Hall calculations.[33] These suggestions were taken as a basis for quantum mechanical descriptions of these systems by Åkesson et al.[12] and Tachikawa et al.[10] without proof. They were later interrogated by Hartmann

Table 2. Results of Geometry Optimization for Rotamers of $[Ti(H_2O)_6]^{3+}$ and $[V(H_2O)_6]^{3+}$

	D_{3d} all horizontal		T_h		D_{3d} all vertical		C_i	
point group	Ti^{III}	V^{III}	Ti^{III}	V^{III}	Ti^{III}	V^{III}	Ti^{III}	V^{III}
ground state	^2E_g	$^3A_{2g}$	^2T_g	^3T_g	$^2A_{1g}$	^3E_g	^2A_g	^3A_g
r(M−O), Å	2.101	2.052	2.098	2.052	2.094	2.049	2.094	2.049
α(O−M-O′)[a]	88.15	87.28	90.0	90.0	87.16	88.78	88.51	89.43
β(O−M-O′)[b]	91.82	92.73	90.0	90.0	92.84	91.20	91.49	90.57
ϕ	−45.0	−45.0	0.0	0.0	45.0	45.0	13.6	−9.4
E,[c] kcal/mol	6.88	3.46	1.99	1.27	2.01	6.90	0.0	0.0

[a] O−M−O′ angle aligned with C_3 axis. [b] O−M−O′ angle perpendicular to C_3 axis. [c] Energy relative to the global minimum structure.

et al.,[16] who found that a C_i structure represents the global minimum on the potential energy hypersurface of the Ti^{III} hexahydrate. The geometry they obtained is identical with our result, which shows that the structure adopted by $[Ti(H_2O)_6]^{3+}$ in the gas phase can be derived from ideal T_h symmetry by relatively small changes. The water planes are rotated by 13.6° from T_h symmetry into the direction of the all-vertical D_{3d} structure accompanied by a slight distortion of the TiO_6 octahedron (O−Ti−O′ angles = 91.5°). If this small angular distortion is neglected, the $[Ti(H_2O)_6]^{3+}$ adheres to S_6 symmetry. This type of arrangement is at variance to the orientations of the coordinated water molecules in a recent neutron diffraction structure analysis of the cesium Ti^{III} alum[30] where a twist angle $\phi = -20.5°$ was found.

Similar results were found for $[V(H_2O)_6]^{3+}$. Again, a structure with C_i symmetry represents the global energy minimum. The deviations from the parent T_h structure are even smaller than for $[Ti(H_2O)_6]^{3+}$ described above. The VO_6 octahedron is less distorted (O−V−O′ angles of 90.6°), and the ϕ angle has a mean value of −10.9°.

In contrast to our findings, experimental structures of various $M[V(H_2O)_6] \cdot 2SO_4 \cdot 6H_2O$ β-alums[29] ($M = K^+, Rb^+, Cs^+$) show S_6 symmetry with ϕ values between −19 and −20°. Thus, the latter structures are closer to the D_{3d} all-horizontal limiting case than the minimum energy structure we obtained. However, detailed comparisons of structures of hexaaqua ions of Ti^{III} and V^{III} in solids in various environments with results from quantum mechanical studies are meaningless if one considers the energy differences between the limiting structures. Table 2 shows the calculated structural and energetic parameters of hexaaqua titanium(III) and vanadium(III) complexes in all possible symmetries. In Figure 2, potential energy curves (electronic ground state)[40] for the coupled rotation of the water planes by leaving the MO_6 body in O_h symmetry are shown for both cases. It is obvious that the found C_i structures are more stable than a T_h arrangement by a neglectable amount of energy. $[Ti(H_2O)_6]^{3+}$ can adopt D_{3d} symmetries when its environment compensates about 2 (all vertical) to 7 (all horizontal) kcal/mol. $[V(H_2O)_6]^{3+}$ in T_h symmetry can be distorted into D_{3d} arrangements with an energy loss of 3 (all horizontal) to 7 (all vertical) kcal/mol. In all alums, short and therefore strong hydrogen bonds dictate the orientations of the water ligands. In the case of β-alums, which is the alum type with planarly coordinating water molecules, the ϕ angles are confined to values between −17 and −22°.[29] In other alums, such as those with guanidinium as the countercation ($\{C(NH_2)_3\}[M(H_2O)_6] \cdot 2SO_4$), ϕ angles close to the D_{3d} all-horizontal limit of −45° are found independent

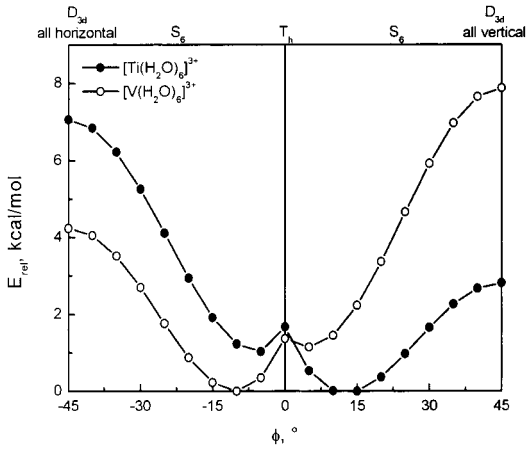

Figure 2. Relative energies of the electronic ground states of $[Ti(H_2O)_6]^{3+}$ and $[V(H_2O)_6]^{3+}$ in S_6 symmetry as a function of the twist angle ϕ (Becke3LYP/6-31+G*, partial geometry optimization by fixing S_6 symmetry at a given ϕ and optimizing the M−O and O−H distances and the H−O−H angles).

Scheme 2. Thermodynamic Cycle Defining Hydration Enthalpies (ΔH_{hyd}) and Free Solvation Energies (ΔG_{solv})

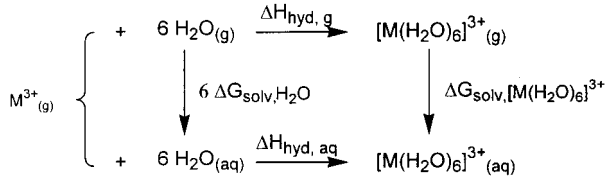

of the type of the metal ion.[37] Thus, the electronic perculiarities of $[M(H_2O)_6]^{3+}$ ions could remain buried if, e.g., only one series of alums is considered. One has to be very careful when deducing detailed electronic influences on geometrical arrangements of these ions from solid-state structures without consideration of the H-bond networks. In addition, there must be a difference to gas-phase structures calculated with quantum mechanical methods.

Gas-Phase and Solvation Energetics. The energetics of formation of aqua complexes are described by the enthalpy differences ΔH_{hyd} (hydration enthalpies) according to the reactions shown in Scheme 2. The values calculated for ΔH_{hyd}(aq) (reaction enthalpy of the transfer of M^{3+} from the gas phase into water, including formation of a hexaaqua complex, lower path in Scheme 2) are compared with experimental data in Table 3. The free-energy changes associated with the transfer of gaseous M^{3+} and $[M(H_2O)_6]^{3+}$ ions into bulk water without complex formation (free energies of solvation, ΔG_{solv}) are also listed in Table 3, together with values of ΔE_b, the overall binding energy for the formation of hexaaqua complexes in the gas phase. The latter is referred to as the same process as ΔH_{hyd}(g) but neglects thermal corrections. The ΔG_{solv} of six water molecules (not listed) and $[M(H_2O)_6]^{3+}$ were

(40) The electronic ground states of d^1 and d^2 systems in T_h symmetry are triply degenerated. This degeneration is suspended when lowering the symmetry. Thus, the potential energy surfaces of A_g and/or E_g states in S_6 symmetry cross at $\phi = 0°$ according to the Jahn−Teller theorem. An observed change in the electronic ground state when changing the sign of ϕ is responsible for the discontinuity of the ground-state curves in Figure 2.

Table 3. Thermodynamic Properties of $[M(H_2O)_6]^{3+}$ in kcal/mol

		$-\Delta G_{solv}$[b]		$-\Delta H_{hyd}$(aq)[c]	
M^{III}	$-\Delta E_b$[a]	M^{3+}	$[M(H_2O)_6]^{3+}$	calcd	exp[50]
Sc	574.36	742.00	444.14	945	931
Ti	625.94	770.68	452.54	1004	993
V	663.33	791.95	454.78	1044	1046
Cr	703.25	810.16	458.07	1087	1099
Mn	701.48	826.92	457.40	1085	1086
Fe	681.61	840.87	453.94	1061	1059

[a] Uncorrected energy difference according to $M^{3+} + 6H_2O \rightarrow [M(H_2O)_6]^{3+}$ in the gas phase. [b] Free energy of solvation in water related to $X^{3+}(g) \rightarrow X^{3+}(aq)$. [c] Standard hydration enthalpy in water according to Scheme 2.

used to obtain ΔH_{hyd}(aq) from ΔH_{hyd}(g) according to the Born−Haber cycle schown in Scheme 2:

$$\Delta H_{hyd}(aq) = H_{[M(H_2O)_6]^{3+}}(g) - H_{M^{3+}{}_g} - 6H_{H_2O_g} + \Delta G_{solv,[M(H_2O)_6]^{3+}} - 6\Delta G_{solv,H_2O}$$

It is therefore necessary to assume that the solvation entropies of these species are equal to each other.[41] The agreement between the calculated and the experimental enthalpies of complex formation in water is impressive and better than previous estimates that were based on different solvent models or cluster approaches.[13−15] Seemingly, interactions between the first and increasingly remote hydrate shells of the metal ions are satisfactorily described by the CPCM method. On the other hand, the ΔG_{solv} values obtained for the complex ions span a range of only 14 kcal/mol, whereas ΔH_{hyd}(g) vary by one magnitude higher. Thus, the calculated solvent effect mainly shifts the ΔH_{hyd}(g) by a near constant amount into the correct direction. The mean value of ΔG_{solv} of the complex ions amounts to -453 ± 5 kcal/mol. It describes the electrostatic interaction between a 3-fold positively charged sphere with a certain radius and a surrounding dielectric (the simple Born equation yields $\Delta G_{solv} = -450$ kcal/mol for an M^{3+} ion with radius of 3.27 Å, which corresponds roughly to the size of hexaaqua ions described by us). The ΔG_{solv} of the naked ions are mainly a function of the ion radius used in the solvent model (see Table 3). They become more negative with rising atomic number. As can be concluded from comparison of values of ΔG_{solv} of the complex ions with the M−O distances in Table 1, variations of the solvent effect on gas-phase energetics are mainly due to variations of their size, too. However, it can also be concluded that the dependence of ΔH_{hyd}(aq) on the type of the metal ion for the described hexaaqua complexes is dominated by its behavior in the gas phase, which is described by ΔH_{hyd}(g) or ΔE_b. So, the following discussion will be based on gas-phase properties.

The dependency of the mean metal−oxygen distances as well as ΔE_b on atomic numbers is shown in Figure 3. The well-known ordering (general lowering of M−O distances and increased exothermicity of complex formation) and increased deviation of these properties from the behavior expected from atomic radii beginning with Ti^{3+} up to Cr^{3+} can be reproduced. According to these data, $[Cr(H_2O)_6]^{3+}$ is the most stable complex in the studied series, and hexahydrated Fe^{III} seems to be near

(41) The assumption $\Delta S_{solv}([M(H_2O)_6]^{3+}) = 6\Delta S_{solv}(H_2O)$ should be valid within the error of the calculations, since solvation entropies describe changes of the solvent structure around a solute when introducing it into the solvent. The water ligands forming the first coordinatively bound hydrate shell of a metal ion should fit into the hydrogen bond network of the solventlike noncoordinated water molecules.

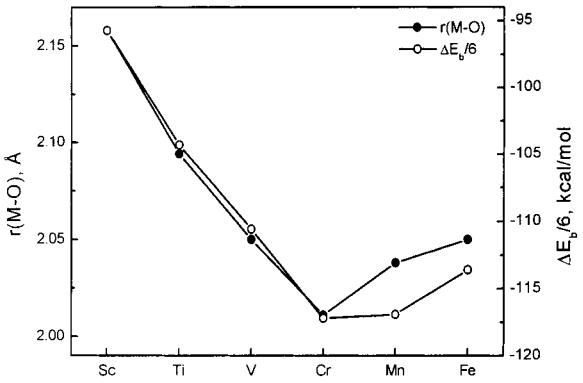

Figure 3. Variation of the mean M−O distances and the gas-phase binding energies ΔE_b of $[M(H_2O)_6]^{3+}$ with atomic number.

similar to V^{III}. The reasons for this behavior will be the subjects of the discussions in the next sections.

Nature of the M−OH$_2$ Bonds: General Trends. The geometrical and thermodynamic features of the 3d $[M(H_2O)_6]^{3+}$ ions that were discussed in the previous sections can be explained from different points of view. From the perspectives of classical LFT, any deviation of thermodynamic parameters from a straight line connecting Sc^{III} (d^0) and Fe^{III} (d^5, high-spin) would be related to differences in the individual LFSE.[1] The LFSE has been introduced to scale the deviations of physicochemical parameters of metal complexes from an ideal stage where the complexes would have a spherical shape. It represents a quantitative measure of energetic effects of a ligand field in a given symmetry that acts on the d electrons of the central ion. Thus, the LFSE is believed to be suitable to judge changes from a regular behavior (e.g., irregular variations of complex stabilities) in cases where the distribution of metal electrons is nonspherical. The LFSE yields good predictions or explanations of observed stabilities of complexes with dominating electrostatic M−L interactions such as hexaaqua ions. In addition, this concept is well-established because of the ease of understanding. On the other hand, really quantitative predictions of complex thermodynamics have to utilize corrections that are not an intrinsic part of the classical LFT. These corrections are mainly due to effects arising from coordinative bonds. That is why it seems to be reasonable to introduce here the description of partially covalent or coordinative M−L bonds by means of quantum mechanical calculations. Settings of the computational results should be delivered eventually in a most transparent way and a commonly understandable language.

The NBO representations of the one-electron density matrices we have chosen contain the common five 3d and one 4s spin−orbital for each electron density of the metal and OH σ-bonds and two electron LPs at oxygen per coordinated water molecule. The two oxygen LPs considered here are one p orbital localized above and below the water plane (with a symmetry suitable for O−M p_π−d_π donation) and one sp hybrid orbital directed along the vector of the water dipole and pointing toward the metal ion (suitable for σ-bonds). The O−H bonds are formed by two sp^3 hybrids at oxygen. This hybridization scheme yields the same geometric possibilities of interaction with the oxygen atom as three sp^2 hybrids.[42] This pure ionic and strictly localized valence bond representation of a hexaaqua complex does not account for the whole electron-density distribution defined by the original one-electron density matrix. Deviations from it become visible as delocalization of electrons from occupied donor orbitals into empty acceptor orbitals. In the systems studied in the present work, the transfer of electron density from the occupied LPs at

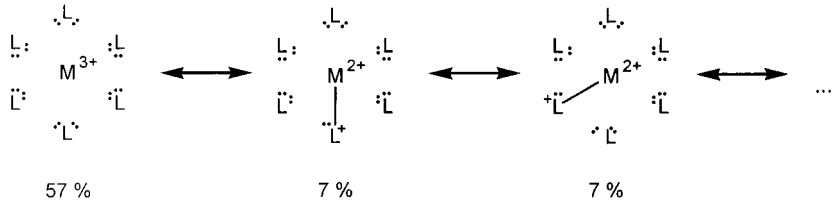

Figure 4. General resonance structure representations (one ionic structure, six structures containing one covalent M−L σ-bond) of $[M(H_2O)_6]^{3+}$. The weights were calculated for $[Sc(H_2O)_6]^{3+}$ via NRT.

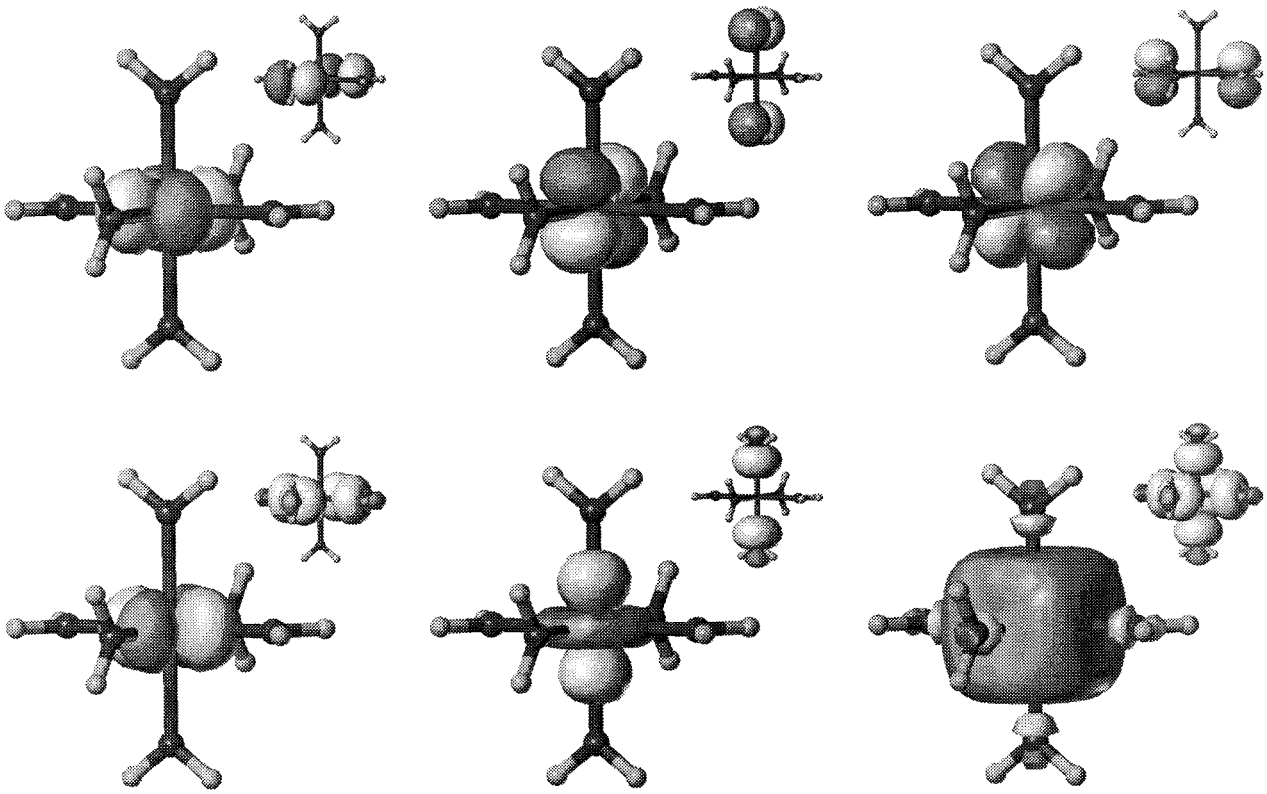

Figure 5. Localized bond orbitals (NBOs) that are responsible for coordinative bonds in the β-density of $[Fe(H_2O)_6]^{3+}$ in T_h symmetry. Large pictures show the five empty 3d and one 4s spin−orbitals at Fe. The insets show the occupied ligand orbitals that transfer electron density into the correponding metal orbital. Upper line: three t_g orbitals and six p LPs at the oxygens, π-bonding. Lower line: two e_g orbitals, one 4s orbital, and six sp LPs at oxygens, σ-bonding.

the oxygen atoms into empty 3d and 4s orbitals of the central ions is the major contribution to electron delocalization. It can be expressed by the resonance structures shown in Figure 4. Combination of the structures by means of natural resonance theory (NRT)[43] for the closed-shell $[Sc(H_2O)_6]^{3+}$ ion reflects the high preference for the ionic structure description. This finding corresponds to the common view of bonding in Werner-type complexes, where only a weak charge transfer contributes to the M−L interactions. The remaining $[M(H_2O)_6]^{3+}$ complexes contain unpaired d electrons. These systems would have to be described by two sets of resonance structures in the unrestricted HF formalism (one set for α spin and one set for β spin). Thus, presentations of resonating Lewis structures seems not to be illuminating enough for reaching a transparent picture. To avoid this split description, we divide the amount of charge transfer into σ- and π-contributions, according to the symmetry of the involved orbitals. Details belonging to this description are illustrated in Figure 5 for the $[Fe(H_2O)_6]^{3+}$ high-spin complex. In general, the NBO representations of all systems studied show similar characteristics. The five 3d orbitals belonging to one-spin orientation split into two groups, both energetically and in relation to the type of corresponding donor orbitals. Three of them (if empty) are lower in energy and accessible for electron density from the p LPs of the oxygen atoms. The remaining two 3d orbitals and the 4s orbital can accept charge mainly from the oxygen sp LPs. Complexes with T_h symmetry show energetic degeneration of the d orbitals that split into three t_g and two e_g orbitals. The two groups are similar to the known sets of t_{2g} and e_g orbitals in a ligand field with O_h symmetry. Structures with lower symmetry do not show this degeneration, but the energetic splitting into two groups and the characteristics of the donor orbitals are retained. So, we will indicate the d orbitals according to O_h symmetry stated above for the sake of clarity. The type of symmetry of a d orbital is accessed by the type of its main electron-donor orbital (mainly sp or p type). This designationis not mathematically correct, but it facilitates the interpretation in the sense of common coordination chemical language. Metal electrons added to the α density in the series

(42) A sp LP is more electronegative than a sp^2 hybrid orbital. Thus, the hybridziation scheme $p + sp + 2sp^3$ of water and oxygen is more appropriate to describe very weak coordinative σ-bonds involving trigonal planar coordinating water than the scheme $p + 3sp^2$. However, an increasing strength of a σ-bond is similar to an increasing p contribution to the sp LP of oxygen. The computational method we used yielded, e.g., $sp^{1.22}$ for $[Cr(H_2O)_6]^{3+}$ (the strongest 3d σ-bonds) and $sp^{0.92}$ for $[Fe(H_2O)_6]^{3+}$ (the weakest 3d σ-bonds).

(43) Glendening, E. D.; Weinhold, F. *J. Comput. Chem.* **1998**, *19*, 593.

Table 4. Contributions to Charge Transfer in $[M(H_2O)_6]^{3+}$ in Electrons

	3d σ^a		3d π^a		4s σ^a			
M^{III}	total	% of Σq	total	% of Σq	total	% of Σq	Σq	$\Delta q_M{}^b$
Sc	0.385	45.4	0.302	35.6	0.161	19.0	0.848	0.862
Ti	0.503	47.3	0.381	35.8	0.180	16.9	1.064	1.049
V	0.640	52.6	0.381	31.3	0.196	16.1	1.217	1.188
Cr	0.814	62.4	0.279	21.4	0.212	16.3	1.305	1.255
Mn	0.724	57.6	0.313	24.9	0.221	17.6	1.258	1.224
Fe	0.440	40.0	0.421	38.3	0.239	21.7	1.100	1.081

[a] Sum of occupation numbers of formally empty metal NBOs with appropriate symmetry. [b] Total charge transfer obtained via NPA.

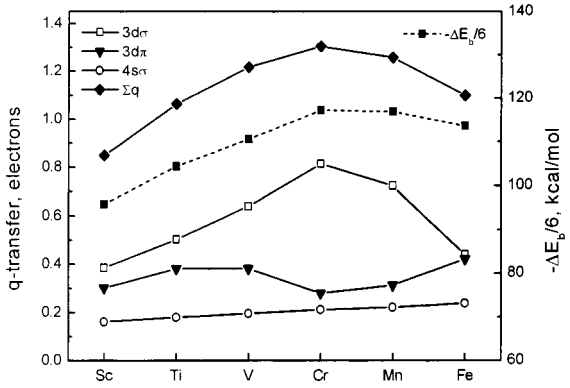

Figure 6. Contributions to charge transfer in $[M(H_2O)_6]^{3+}$.

from Sc^{3+} to Fe^{3+} successively fill the t_{2g} orbitals and then the e_g orbitals, yielding high-spin complexes with empty β orbitals. The d orbitals with β spin can accept electron density from ligand orbitals with proper symmetry, even if the corresponding α orbital is occupied. We obtained the total amount of negative charge transferred from the ligands to the metal ion by summation of occupation numbers of formally empty metal orbitals in both densities. According to their symmetries, we divide it into σ- and π-contributions to obtain a quantitative measure (one number for each type of bond) for a bonding model (cf. Table 4 and Figure 6). In the case of molecules with low symmetry, this separation and orbital indication is not exact because the canonical MOs forming the original wave function are not restricted to the symmetry of the participating AOs at the metal. This yields a mixture of all AOs in the NAO basis, forming a d orbital in the NBO basis. In addition, the orbitals of the t_{2g} set become able to accept electron density from the sp hybrids at the oxygens. On the other hand, the obtained energetical grouping of localized d orbitals is very clear, and the contribution of overlaps of orbitals with the wrong symmetry is negligible. Therefore, our utilization of occupation numbers of groups of metal orbitals seems to be rather beneficial for the discussion of trends. Also, the total amount of charge transfer obtained in this way (Σq in Table 4) is virtually identical with the loss of positive charge at the central ion (Δq_M in Table 4). The latter quantity was obtained via population analysis of the natural atomic orbitals (NAOs, natural population analysis[44]). The agreement between these two numbers shows that delocalization of metal electrons into empty antibonding orbitals at the ligands and 4p metal orbitals does not contribute significantly to the M−L interaction in these cases. Otherwise, a significant amount of electron density would be found in localized Rydberg orbitals originating from higher functions of the original basis set that are not considered by our analysis. We are therefore convinced that the procedure presented here is useful in the analysis of trends in variations of complex geometries and thermodynamic parameters in dependence of metal complex d electron configurations.

M−OH$_2$ Bonding in $[Sc(H_2O)_6]^{3+}$ to $[Fe(H_2O)_6]^{3+}$. Figure 5 illustrates the description of complex structure in terms of localized orbitals for the iron complex. The quantities collected in Table 4 are plotted vs the atomic number in Figure 6. A comparison between Figure 6 and Figure 3 shows that the quantities ΔH_{hyd}, the M−O distances, and Σq vary with atomic numbers in quite the same way, showing an extremum at Cr^{III} and hexahydrated Fe^{III} in between Ti^{III} and V^{III}. The trend in Σq is clearly dominated by the altering occupations of the e_g-like orbitals (3d σ-bonds). A smaller influence on Σq results from the variations of the bonding interactions with the t_{2g}-like orbitals (3d π-bonds) and the 4s orbital (4s σ-bonds). The average amount of charge transferred per oxygen donor is about 0.2 electron. The appropriate contributions to Σq are 50% from 3d σ-, 30% from 3d π-, and 20% from 4s σ-bonding interactions. These contributions show certain variations. $[Cr(H_2O)_6]^{3+}$ shows the largest amount of charge transfer. Σq is made up by more than 60% from 3d σ-bonding and only 20% from 3d π-bonding. $[Fe(H_2O)_6]^{3+}$ behaves differently. Here, only 40% of Σq comes from 3d σ-bonding. Now the influence from 3d π-bonding has increased to 38% such that 3d σ- and π-interactions operate with practically equal extents. It is also interesting to mention at this point that the plot of the 3d π-interactions has a sigmoidal shape and these varying percentages of 3d π-interactions contained in Σq lead to the differences in shape between the Σq- and 3d σ-plots in Figure 6. Therefore, and not unexpected, Fe^{III} is the best π-acceptor among these ions, in agreement, e.g., with the highly stabilized Fe^{III} complexes where the strongly π-donating catecholato oxygen acts as a donor atom.[45]

For the reason of comparison with hypervalent transition metal hydrides or carbenes that were extensively studied with the NBO method,[8] we briefly describe coordinative bonds in hexaaqua complexes also by means of the metal character of localized oxygen LPs in the basis set of natural localized molecular orbitals (NLMOs). Each sp LP at oxygen has about 4.5 (Sc^{III}) to 8% (Fe^{III}) metal character. The contribution of metal d orbitals to one p LP in the NLMO basis amounts to 2.3% in the Sc^{III} complex and reaches 6.5% at iron. These numbers again reveal that these complexes are characterized by extremely polar coordinative bonds with dominating σ-character. That is why hexaaqua ions belong traditionally to the domain of classical LFT or the angular overlap method (AOM). Metallorganic compounds show covalent M−L bonds with about 30−60% metal character,[8] so they are best described by valence bond models.

The extent of electron donor−acceptor interactions generally depends on three conditions: (i) the potential (or ability) of the acceptor orbital to obtain electron density, (ii) the donor potential of the donor orbital, and (iii) other circumstances that prevent these two potentials from being fully utilized, such as geometric arrangements, etc. These potentials are usually measured in quantities such as electronegativity, ionization potentials (IP), or electron affinities (EA). It is possible to apply a simplified and qualitative view here on the basis of the electron affinities of the naked metal ions in individually operating high-spin electron configurations. This idea was originally rationalized by Williams.[5] The potential of a metal 4s orbital to accept

(44) Reed, A. E.; Weinstock, R. B.; Weinhold, F. *J. Chem. Phys.* **1985**, *83*, 735.

(45) Karpishin, T. B.; Gebhard, M. S.; Solomon, E. I.; Raymond, K. N. *J. Am. Chem. Soc.* **1991**, *113*, 2977.

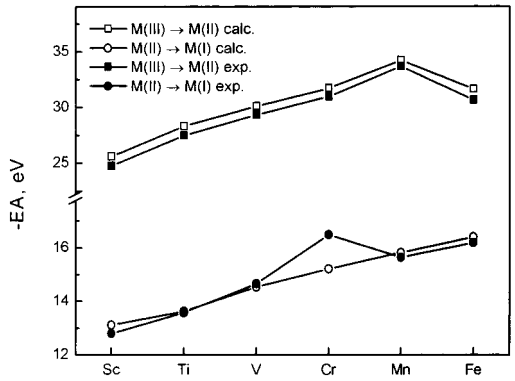

Figure 7. Calculated and experimental[51] electron affinities of M^{2+} and M^{3+}.

electron density can be related to the electron affinity of M^{2+} (equal to the negative IP of M^+, upper row in Scheme 1). The electron acceptor strength of metal d orbitals can be described by the lower row in Scheme 1 (electron affinity of M^{3+}, equal to the negative ionization potential of M^{2+}). Theoretical values have been calculated for EAs of Sc^{2+} to Fe^{2+} and Sc^{3+} to Fe^{3+} to prove the reliability of our computational method related to electron acceptor strengths of metal ions and because only the experimental EA of Sc^{2+} and Mn^{2+} are related to the $3d^n\ 4s^1$ configuration of M^+ as needed. For the remaining M^+, the $3d^{n+1}\ 4s^0$ state is preferred.[46] Figure 7 summarizes the experimental and calculated data. The level of theory we applied is in principle not appropiate for the calculation of quantitatively accurate IPs or EAs because of the single determinant description of degenerated states. Nevertheless, the agreement to the experimental trends in the case of the EA of M^{3+} is surprising. As expected, the absolute amount of the EA of an empty 4s orbital increases continuously with increasing atomic number (lower plot in Figure 7), caused by the increasing electron−nuclear attraction as everywhere in the periodic system. Within the studied series of hexaaqua ions, a straight line is observed, similar to the charge transferred into the 4s orbital in the hexaaqua complexes (see Figure 6). So, this contribution to charge transfer (about 20%) is completely independent of ligand field effects. The way in which the EAs of the 3d orbitals change (upper plot in Figure 7) is similar in shape to the EAs of the 4s orbital up to manganese. In the case of iron, a drop has to be noted. The growing part of this plot is caused by the same reason as described for the 4s orbitals. The low EA of Fe^{3+} has to be explained in terms of spin pairing along the $d^5 \rightarrow d^6$ interconversion. The well-established rules of variations of thermodynamic properties in the periodic system of elements can be related qualitatively to the EAs of metal d orbitals influenced by a ligand field, too. The EA of the t_{2g} set in an octahedral field should increase from Sc^{3+} (d^0) to V^{3+} (d^2), yielding an increased amount of π-bonding. Indeed, this is found qualitatively by the NBO analysis (see Figure 6). The increase, however, is not as high as expected when comparing Ti^{3+} with V^{3+}. They show near similar amounts of π-bonding. The reasons for the apparent identity in π-acceptor behavior between Ti^{III} and V^{III} will be further outlined below. The increase of the number of electrons when going from V^{3+} to Cr^{3+} (d^3) is connected with the expected decrease in π-acceptor strength (cf. Figure 6), because spin pairing has to occur when additional charge density is transferred into the t_{2g} (O_h) orbitals. By further increasing the number of metal d electrons when going from Cr^{3+} to Mn^{3+} (d^4) and Fe^{3+} (d^5), spin pairing also has to occur when π-bonds are formed, but the EA of the t_{2g} orbitals should rise as compared to Cr^{3+} because the nuclear charge rises. This seems to be the reason for our finding that Fe^{3+} in its hexaaqua complex reaches π-transfer similar to V^{3+} (see Figure 6). The variation of σ-accepting abilities can be explained in a similar way when focusing on the e_g (O_h) orbitals. It is expected here that their EAs should continuously increase from the d^0 (Sc^{III}) to the d^4 (Mn^{III}) case, and a decrease should take place only as a result of spin pairing at d^5 (Fe^{III}). So the Sc^{3+} ion is expected to be the weakest σ-acceptor, and Mn^{3+} should show the strongest 3d σ-bonds. Whithin the current series of hexaaqua complexes, this assumption is not validated. We find Cr^{3+} to be the best acceptor of 3d σ-density.

It is possible at this point to summarize the observations about charge-accepting potentials of the different types of metal orbitals and actual use of them in the $[M(H_2O)_6]^{3+}$ complex ions. We note a general agreement between the variations of the electron affinities and the individual bonding contributions. The calculated strength of coordinative σ- and π-bonds in the complexes are in line with the well-established rules of the periodic system. Exceptions are the σ-accepting potential utilized actually by Mn^{3+}, and the unexpected similar π-accepting behavior of Ti^{3+} and V^{3+}. Since these complexes are subject to the Jahn−Teller effect, it is straightforward to discuss their unusual behavior regarding charge transfer by means of their M−L interactions in different symmetries.

Within this context, the behavior of Mn^{III} can be explained easily. As stated above, a T_h symmetric complex leads to a ^5E_g ground state. It is characterized by degenerated e_g orbitals, or in other words, the e_g electron can be found in each of them with the same probability. This yields σ-repulsion to all six sp LPs at oxygen. It can be minimized by axial compression or elongation of the MO_6 octahedron, corresponding to a change of the electronic ground state and putting the e_g electron in only one e_g orbital. However, the possibility to form coordinative σ-bonds is reduced. The localization procedure we used yields the e_g electron in the dz^2-like orbital; thus, the number of water molecules that act as σ-electron donors to the remaining empty e_g orbital in the α-density reduces from six to four. It should be reasonable to relate the drop of σ-electron density transferred to the e_g set in this complex to this reduced number and not to an apparently low acceptor potential of the metal ion. Moreover, the observation of the rather strong acidity of $[Mn(H_2O)_6]^{3+}$ ($pK_{a1} = -0.6$[47]) in contrast to other group members such as $[V(H_2O)_6]^{3+}$ ($pK_{a1} = 2.6$)[48] or $[Fe(H_2O)_6]^{3+}$ ($pK_{a1} = 2.5$)[49] also support the conclusion that Mn^{3+} has the intrinsic possibility to accept a huge amount of charge density, but it is not utilized in the hexaaqua complex for steric reasons. This conclusion implies the presupposition that the portion of the M−L interaction energy that originates from coordinative bonds is small as compared to the electrostatic and steric parts.

Detailed Description of Bonding in $[Ti(H_2O)_6]^{3+}$ and $[V(H_2O)_6]^{3+}$. As shown in the preceding sections, the calculated

(46) Russo, T. V.; Martin, R. L.; Hay, P. J. *J. Chem. Phys.* **1994**, *101*, 7729.
(47) *NIST Critical Stability Constants and Related Thermodynamic Constants of Metal Complexes*, Version 5.0; NIST Standard Reference Databases; National Institute of Standards and Technology: Gaithersburg, MD, 1998.
(48) Meier, R.; Boddin, M.; Mitzenheim, S.; Kanamori, K. In *Metal Ions in Biological Systems*; Sigel, H., Sigel, A., Eds.; M. Dekker: New York, 1995; Vol. 31, Chapter 2, p 45.
(49) Flynn, C. M., Jr. *Chem. Rev.* **1984**, *84*, 31.
(50) Smith, D. W. *J. Chem. Educ.* **1977**, *54*, 540.
(51) *CRC Handbook of Chemistry and Physics*, 75th ed.; Lide, D. R., Frederikse, H. P. R., Eds.; CRC Press: Boca Raton, FL, 1984.

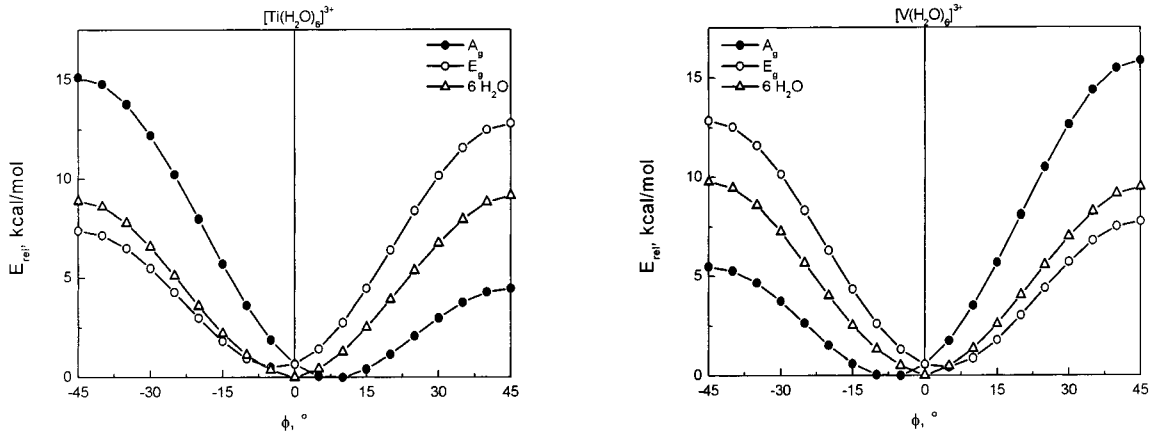

Figure 8. Relative energies of the two lowest lying electronic states of $[Ti(H_2O)_6]^{3+}$ and $[V(H_2O)_6]^{3+}$ with varying ϕ in S_6 symmetry (CASSCF results using geometries as described for Figure 2) and relative energies of the $(H_2O)_6$ subunit.

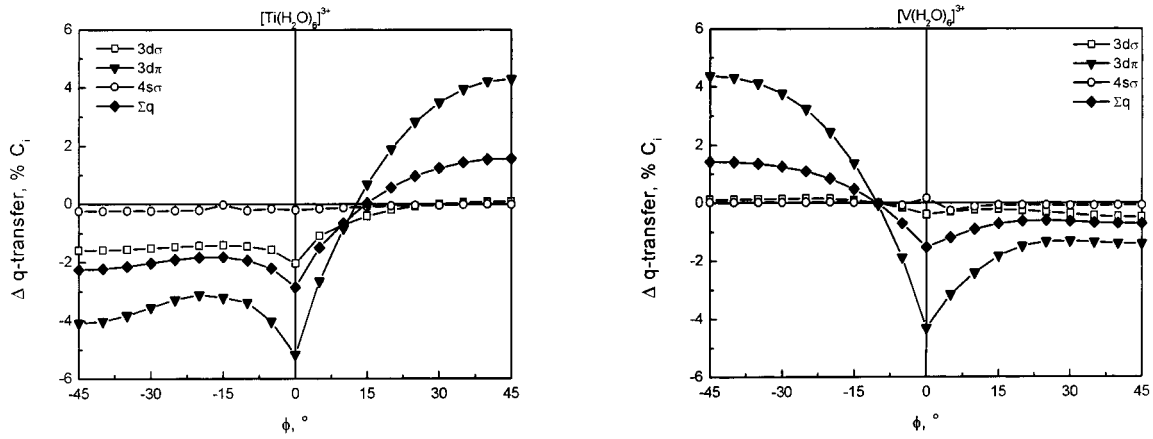

Figure 9. Changes of contributions to charge transfer in the electronic ground state of $[Ti(H_2O)_6]^{3+}$ and $[V(H_2O)_6]^{3+}$ when varying ϕ in S_6 symmetry (B3LYP/6-31+G*). The numbers are relative differences to the contributions in the global minimum structures (C_i symmetry).

geometric and thermodynamic properties of the Sc^{III}−, Cr^{III}−, Mn^{III}−, and Fe^{III}−hexaaqua complexes can be explained on the basis of orbital electron affinities. In the case of $[Ti(H_2O)_6]^{3+}$ and $[V(H_2O)_6]^{3+}$, additional questions arise as follows: (i) What is the reason for the observed symmetry change from T_h to a C_i structure, which is similar to the parent T_h structure? (ii) Which influences prevent these systems from forming D_{3d} symmetric arrangements as postulated by Cotton et al.?[33] (iii) Why does hexahydrated Ti^{III} seemingly tend to a D_{3d} all-vertical structure (positive value of ϕ, see Figure 2), whereas the hexahydrate of V^{III} tends to a D_{3d} all-horizontal arrangement (negative value of ϕ)? (iv) Which influences are responsible for the almost equal π-acceptor behavior of Ti^{III} and V^{III} in their hexaaqua complexes?

These questions can be answered by a detailed analysis of the variations of M−L and L−L interactions when varying ϕ from −45 to +45°. The corresponding potential energy curves of the electronic ground states of $[Ti(H_2O)_6]^{3+}$ and $[V(H_2O)_6]^{3+}$ were already shown in Figure 2. Figure 8 shows the potential energy curves for the two lowest lying states of these complexes as obtained from state-averaged CASSCF calculations and the relative energy of the coordination sphere $(H_2O)_6$ without the central ion. In Figure 9, we display the difference between the amounts of charge transfer at a given ϕ and at the minimum-energy C_i structure in the electronic ground state normalized to the absolute amount of charge transfer in C_i geometry. A negative value means a smaller amount of charge transfer at a given ϕ, as compared to the global minimum structure. This quantity allows the plotting of variations of all bonding contributions in one figure. As concluded from the energy of the ligand framework (see Figure 8), water interactions are optimal at $\phi = 0°$, whereas both D_{3d} arrangements are energetically unfavored, as expected. Without considering the M−L interactions, these complexes should form T_h symmetric structures like d^0, d^3, and d^5 complexes in the series do. An analysis of the amounts of charge transfer (cf. Figure 9) reveals a strong dependency of π-bonding on ϕ, whereas σ-bonding is less influenced. The weakest charge transfer in the electronic ground state is obtained for $\phi = 0°$. This finding is a representation of the molecular basis of the Jahn−Teller effect. The same explanation, as already given for the manganese complex, can be applied here. A triply degenerated ground state of $[Ti(H_2O)_6]^{3+}$ and $[V(H_2O)_6]^{3+}$ is coupled with equal probabilities to find the metal electron(s) in each of the t_g (T_h) orbitals, yielding repulsion to all six p LPs at the oxygen atoms and no possibility to form π-bonds in the electron density with α-spin. Thus, $\phi = 0°$ is favored by interligand interactions but not by M−L interactions. The resulting geometric arrangement is a compromise between these two influences. The direction of resulting geometry changes is related to the possibilities to maximize the amount of π-bonding. The general conclusion given by Cotton et al.[33] that Ti^{III} shows maximal π-bonding at $\phi = 45°$, whereas V^{III} shows strongest π-bonds at $\phi = -45°$ is supported by our calculations. These findings deliver the answers on questions (i) and (ii) given above.

Obviously, the tendency of Ti^{III} and V^{III} to favor geometries with a particular sign of ϕ (question iii) is coupled with the extent of π-bonding (cf. Figure 9). This behavior can be

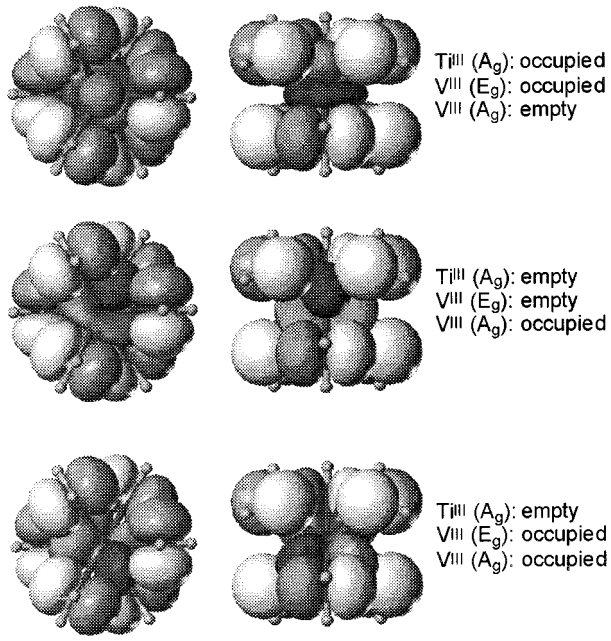

Figure 10. Three t_{2g}-like orbitals of Ti^{III} and six p LPs at oxygen in D_{3d} all-vertical symmetry ($\phi = 45°$). Left column: view into the direction of the C_3 axis. Middle column: view perpendicular to the C_3 axis. Right column: electron configuration including different states of V^{III}.

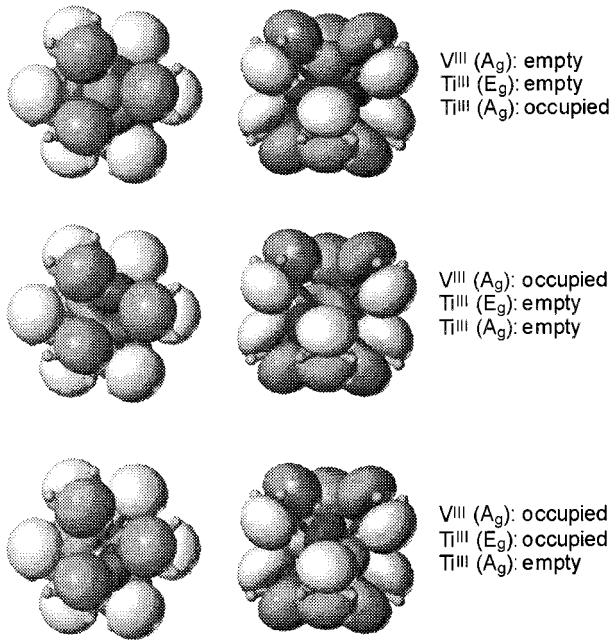

Figure 11. Three t_{2g}-like orbitals of V^{III} and six p LPs at oxygen in D_{3d} all-horizontal symmetry ($\phi = -45°$). Left column: view into the direction of the C_3 axis. Middle column: view perpendicular to the C_3 axis. Right column: electron configuration including different states of Ti^{III}.

illustrated by plots of the corresponding NBOs. Figure 10 shows the t_{2g}-like orbitals together with all p LPs for $[Ti(H_2O)_6]^{3+}$ at $\phi = 45°$ (D_{3d} all vertical, A_g state). The vanadium complex with $\phi = 45°$ yields the same shape and orientation of these orbitals. The orbital containing the d electron of Ti^{III} (upper line in Figure 10) corresponds to the empty t_{2g}-like orbital in the A_g state of V^{III}. This orbital has an orientation with minimal overlap to the p LPs of the water oxygens. It yields minimal repulsion to the p LPs in $[Ti(H_2O)_6]^{3+}$ but also minimized π-bonding in $[V(H_2O)_6]^{3+}$. The amount of π-transfer in $[V(H_2O)_6]^{3+}$ observed at this geometry in the A_g state (result not shown) is lower than found in T_h symmetry. Figure 11 shows the same orbitals for $[V(H_2O)_6]^{3+}$ at $\phi = -45°$ (D_{3d} all horizontal, A_g state). Again, these orbitals look similar for $[Ti(H_2O)_6]^{3+}$ at $\phi = -45°$. The orbital containing the t_{2g} electron hole of V^{III} (upper line in Figure 11) shows maximal overlap with the p LPs at oxygen, corresponding to a maximum of π-bonding. The same orbital contains the d electron at Ti^{III} in its A_g state, yielding a maximum of steric repulsion. Thus, the preference of both complexes for a particular sign of ϕ (Ti^{III}, positive; V^{III}, negative; question iii) can be understood on the basis of avoided repulsion between occupied metal t_{2g}-like orbitals and p LPs at oxygen on one hand and π-bonding on the other. The change of the electron configuration at unfavored geometries for $[Ti(H_2O)_6]^{3+}$ at $\phi < 0$, and for $[V(H_2O)_6]^{3+}$ at $\phi > 0$ (see comments in Figures 10 and 11) yields a partial compensation of adverse steric contacts by possibilities for π-bonding but, unfortunately, also to degenerated ground states in S_6 symmetry. Since apparent local potential energy minima at $\phi \approx -5°$ ($[Ti(H_2O)_6]^{3+}$, E_g ground state) and $\phi \approx +5°$ ($[V(H_2O)_6]^{3+}$, E_g ground state) were observed in S_6 symmetry (see Figure 2), there exists the possibility that true local minima can also be found when leaving O_h symmetry of the MO_6 body at these angles. These arrangements would belong to the C_i or C_1 point groups, which fulfill the Jahn−Teller theorem. We were unable to locate such minima by geometry optimization. This finding is a tribute to the flatness of the potential energy hypersurfaces in this region and to the small energy gap between the lowest electronic states, which complicates quantum mechanical calculations.

However, repulsion between occupied metal orbitals and p LPs at oxygen obviously dominates the M−L interaction in these two cases, as compared to the contribution of coordinative bonds. It seems reasonable, therefore, to extend the conclusion regarding anisotropic σ-bonding in $[Mn(H_2O)_6]^{3+}$ given above to π-bonding in $[Ti(H_2O)_6]^{3+}$ and $[V(H_2O)_6]^{3+}$ (question iv). If the nuclear charge would be the only factor controlling the extent of $O-M^{III}$ π-donation, a π-acceptor potential of V^{III} higher than that of Ti^{III} is expected. This potential, however, cannot be utilized fully in the hexaaqua−V^{III} complex because the need to avoid $\pi-\pi$-repulsions leads to a smaller degree of spatial freedom for $O-V^{III}$ $p_\pi-d_\pi$ bonding as compared to Ti^{III}. Therefore, it is possible to predict that only those oxygen containing ligands should form very stable V^{III} complexes where the ligand backbones are flexible enough to ascertain that $O-V^{III}$ $p_\pi-d_\pi$ bonding takes place only with the sole unoccupied t_{2g} (O_h) orbital.

This conclusion is in good agreement with our experimental findings for V^{III} complex stabilities with a larger number of oxygen containing ligands.[7] In the latter study, it was found that edta (ethylenediaminetetraacetato) is a ligand that fulfills the special requirements of optimal bonding to V^{III} such that the formation constant of V^{III}−edta ($\log \beta = 26.4$) is even larger (by more than 1 order of magnitude) than the analogous value of Fe^{III}−edta ($\log \beta = 25.0$).[47] The ligand tmdta (trimethylenediaminetetraacetate), on the other hand, is not flexible enough to satisfy the special coordination requirements of V^{III}. In this case, the formation constant ($\log \beta = 18.5$) is more than 7 orders of magnitudes smaller than that for V^{III}−edta and also significantly lower than that of Fe^{III}−tmdta ($\log \beta = 21.4$).[47]

It can also be concluded on the basis of Figures 2 and 9 that the intrinsic preference of $[Ti(H_2O)_6]^{3+}$ and $[V(H_2O)_6]^{3+}$ for a particular sign of ϕ can be overridden by counterbalancing

effects (e.g., by strong hydrogen bond networks in solid-state complexes) because of the small difference in energy between the complex geometries in the vicinity of T_h symmetry.

Summary

The NBO representation of simple transition metal complexes such as $[M(H_2O)_6]^{3+}$ enabled us to elucidate the geometrical and energetical features that guide the bonding in this archetypical and important class of transition metal complexes. Although simple on a first view, it turns out that various counterbalancing effects need to be analyzed. Eventually, the nature of bonding in the individual $[M(H_2O)_6]^{3+}$ members of the group of 3d ions from Sc^{III} to Fe^{III} could be expressed in a language common to most chemists.

Basically, the DFT/NBO analysis of the charge-transfer contributions to the overall M−L interactions leads to similar results as those obtained by classical LFT. In contrast to the terminology used in LFT, we were able to explain the trends in the bonding interactions and thermodynamic features by means of simple rules usually applied in the periodic table. Such an approach seems to be more suitable for the analysis of the thermodynamics of more sophisticated systems such as chelate complexes.

Acknowledgment. We are pleased to thank Thomas Ritschel (University of Potsdam) for the setup and discussion of the CASSCF calculations presented in this work.

IC001258T